Nature of exciton transitions in hexagonal boron nitride

J. Li,[1] X. K. Cao,[1] T. B. Hoffman,[2] J. H. Edgar,[2] J. Y. Lin,[1] and H. X. Jiang[1,a)]
[1]*Department of Electrical and Computer Engineering, Texas Tech University, Lubbock, Texas 79409, USA*
[2]*Department of Chemical Engineering, Kansas State University, Manhattan, Kansas 66506, USA*

(Received 15 January 2016; accepted 9 March 2016; published online 22 March 2016)

In contrast to other III-nitride semiconductors GaN and AlN, the intrinsic (or free) exciton transition in hexagonal boron nitride (*h*-BN) consists of rather complex fine spectral features (resolved into six sharp emission peaks) and the origin of which is still unclear. Here, the free exciton transition (FX) in *h*-BN bulk crystals synthesized by a solution method at atmospheric pressure has been probed by deep UV time-resolved photoluminescence (PL) spectroscopy. Based on the separations between the energy peak positions of the FX emission lines, the identical PL decay kinetics among different FX emission lines, and the known phonon modes in *h*-BN, we suggest that there is only one principal emission line corresponding to the direct intrinsic FX transition in *h*-BN, whereas all other fine features are a result of phonon-assisted transitions. The identified phonon modes are all associated with the center of the Brillouin zone. Our results offer a simple picture for the understanding of the fundamental exciton transitions in *h*-BN. © *2016 AIP Publishing LLC*.
[http://dx.doi.org/10.1063/1.4944696]

BN has many known phases including cubic, wurtzite, and hexagonal structures. Among these, hexagonal is the stable phase for materials produced at atmosphere pressure at any growth temperatures.[1,2] Besides important practical applications, hexagonal BN (*h*-BN) is also a unique wide bandgap semiconductor for studying the fundamental properties as it is the only layer-structured semiconductor among III-nitride semiconductors and also the only wide bandgap semiconductor ($Eg > 4$ eV) among layer-structured (or two-dimensional) materials. With an energy bandgap around 6.5 eV, *h*-BN is emerging as an important semiconductor material.[3–7] With its unique physical properties including high temperature and chemical stability, *h*-BN has potential applications in high temperature/power electronic device applications. P-type conductivity seems to be more easy to realize in *h*-BN than in AlN, which reveals the potential of *h*-BN for deep UV emitter and detector applications.[7,8] With its large thermal neutron cross-section, *h*-BN is also a promising material for realizing high efficiency and low cost solid-state neutron detectors.[9,10]

Our knowledge concerning the band structure and optical properties of *h*-BN is limited. In spite of the recognition of the importance of *h*-BN for emerging applications, many of its fundamental physical properties are still unknown. For example, the detailed band structure parameters of *h*-BN are still unclear. The experimental band gap was determined in the past only by optical absorption, transmission, and indirectly from photoluminescence (PL) lifetime measurements with values scattered around 6 eV at low temperatures.[11–13] The band-edge transitions in *h*-BN are distinctly different from that of wurtzite (w)-AlN having a comparable energy bandgap ($Eg = 6.1$ eV at 10 K).[14] Fundamental optical transitions including the nature of the intrinsic or free exciton transitions in *h*-BN are not yet well understood. Both the free exciton (FX) transition (denoted as S-series lines[15]) and impurity-bound (or trapped) exciton transition (denoted as D-series lines[15]) possess rather complicated spectral features. For instance, the S-series lines of the FX transition consist of six sharp emission lines above 5.75 eV (Refs. 13 and 15), and the origin of which is still debated. The fine features have been thought to arise from the doubly degenerated dipole-forbidden (dark excitons with lower emission energies) and dipole-allowed (bright excitons with higher emission energies) exciton states, in which the dark exciton state could become allowed either due to the spontaneous or symmetry breaking caused by energy transfer from bright exciton as a result of the zero-point vibration of the lattice,[16,17] or a strong spin–orbital interaction due to 2D layered structure.[18,19] It is, therefore, of fundamental and technological importance to fill in the unknowns for *h*-BN.

Recently, much progress has been made in the growth of *h*-BN in the forms of bulk crystals by high temperature/high pressure (HT/HP)[4,5,15] as well as by solution techniques[3,13] and epilayers by metal organic chemical vapor deposition (MOCVD).[7–10] Epitaxial *h*-BN layers with high optical qualities can be achieved,[7,20] but these materials generally lack the intrinsic FX transitions above 5.7 eV due to the presence of native and point defects.[7,20] Most recent studies have suggested that the D-series emission lines are due to the recombination of excitons bound to deep acceptors formed by carbon impurities occupying the nitrogen sites, and *h*-BN epilayers exhibiting pure intrinsic FX emission can be obtained by growing the materials under high ammonia flow rates.[21] However, the detailed features of the FX transitions in *h*-BN epilayers are distinctly different from those in *h*-BN bulk crystals,[21] which is what remains to be investigated and understood. Currently, bulk *h*-BN crystals are small (less than 1 mm by 1 mm),[3–5,13,15] but the basic properties measured from the bulk materials set the benchmarks for the further development of wafer scale epilayers. Here, we report the properties of the FX transition and strong exciton–phonon coupling in *h*-BN bulk crystals probed by time-resolved

a)hx.jiang@ttu.edu

PL spectroscopy. By comparing the experimental and calculation results, we suggest a simple picture for the understanding of the FX transition in *h*-BN bulk crystals. The results also reveal significant differences between *h*-BN and w-AlN in their fundamental optical properties.

Bulk *h*-BN materials employed in this study were synthesized by precipitation using nickel (Ni) and chromium (Cr) solvent mixture at atmospheric pressure. The source material was hot pressed *h*-BN powder. The source material was soaked at a temperature of 1525 °C for 6 h and, subsequently, cooled at a slow rate of 4 °C per hour until solvent solidification. The cooling rate has to be slow enough to precipitate high quality crystals. Growth conditions were also discussed elsewhere.[22] The inset of Fig. 1 shows an optical microscope image of a bulk *h*-BN crystal on Ni/Cr substrate with a typical dimension of about 250 μm across and 30 μm thick. Figure 1 shows an X-ray diffraction (XRD) θ-2θ scan of *h*-BN (002) reflection plane with a peak at 26.8°, which is in a good agreement with the literature value.[23] The observed *h*-BN (002) peak has a full-width at half-maximum (FWHM) of around 600 arc sec, which implies that there are some orientation variations of the c-planes in the crystal. Larger crystals as long as 900 μm were also obtained on the same growth, but the optical qualities are generally not as good as those of smaller size crystals. A deep UV time-resolved PL system was utilized to probe the emission properties.[13,20] The system consists of a frequency quadrupled 100 fs Ti:sapphire laser providing an excitation photon energy of 6.28 eV and a monochromator (1.3 m) in conjunction with a single photon counting detection system providing a time-resolution of 20 ps and a streak camera system providing a time-resolution of 2 ps.

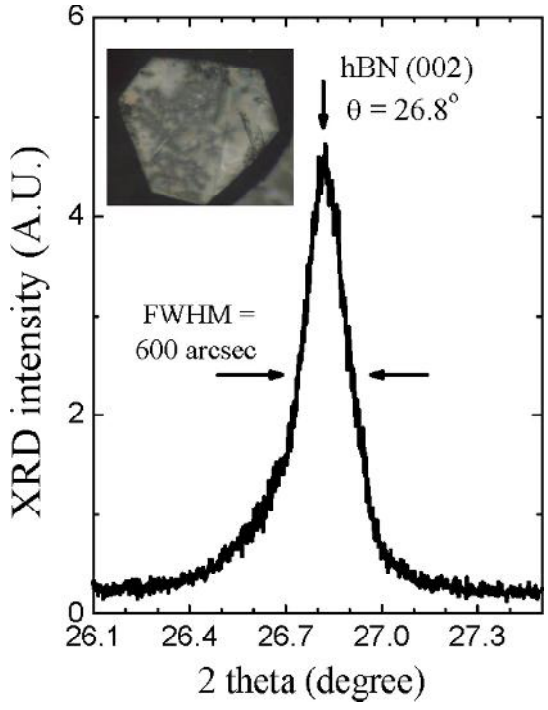

FIG. 1. X-ray diffraction (XRD) θ-2θ scan of the *h*-BN (002) reflection peak of the bulk crystal used in this study. The inset is an optical image of the *h*-BN bulk crystal sample used in the present study.

The exciton PL emission spectrum measured at 10 K is shown in Fig. 2(a), which exhibits similar fine features as those reported for *h*-BN bulk crystals grown by a HT/HP technique[15] and comprises both the FX transition (S-series) and impurity-bound exciton transition (D-series) lines. In contrast to *h*-BN bulk crystals grown by a HT/HP technique which generally exhibit smaller D-series peaks than the S-series peaks,[15] the emission intensities of the S-series lines are smaller than those of the D-series lines in our samples, an indicative that bulk *h*-BN crystals synthesized by precipitation contain higher concentrations of impurities/defects than HT/HP grown materials. In comparison with PL spectra of AlN,[14] the exciton transitions in *h*-BN are quite complicated. As shown in Fig. 2(b), six sharp emission lines have been resolved between 5.75 and 5.90 eV. All these transition lines have been ascribed to the intrinsic or FX transitions and labeled as S-series lines.[13,15] One of the possibilities is that these emission lines correspond to the exciton transitions involving different splitting bands such as A, B, and C valance bands in AlN and GaN.[14,24] However, the relative emission intensities of the excitonic transitions involving different splitting bands are related to the density of states (DOS) of the respective bands, decay characteristics, and the statistical distributions of [exp(−ΔE/kT)], where ΔE is the energy difference between the two bands and T is the measurement temperature. However, the relative emission intensities among these transition lines measured at 10 K do not support this interpretation. For instance, if 5.771 and 5.799 eV emission lines were due to the recombination of excitons involving different splitting bands with an energy separation of 28 meV, the relative emission intensity of the 5.799 eV line should be only a factor of $\exp[-28/kT(=10\,K)] \sim 7 \times 10^{-13}$ of that of the 5.771 eV line, assuming that the DOS and decay characteristics are comparable for these two bands. This is obviously not the case, and therefore, the possibility of the multiple exciton transition lines involving the splitting bands can be precluded.

By carefully inspecting the PL spectrum shown in Fig. 2(b), one can observe that there is a similarity between emission lines at 5.799 (S3) and 5.771 eV (S4) as well as between 5.791 (S3t) and 5.763 eV (S4t). Significantly, the energy difference between the emission lines of 5.897 (S1) and 5.869 eV (S2) is about 28 meV, which equals to the difference between the 5.799 (S3) and 5.771 eV (S4) lines. There are also similarity between 5.897 (S1) and 5.799 (S3) eV emission lines as well as between 5.869 (S2) and 5.771 (S4) eV emission lines. If we cut a portion of the PL spectrum between 5.70 and 5.82 eV and shift it by 98 meV to the higher energy side, we immediately recognize that the two groups of emission lines at 5.897 (S1)/5.869 (S2) eV and 5.799 (S3)/5.771 (S4) eV have similar characteristics and are clearly related. By repeating the same analysis, we can identify that various lines in the S-series are in fact correlated. Furthermore, the decay lifetime measurement results also suggest that these emission lines are correlated. Figure 3 shows the PL decay kinetics of two representative emission peaks at 5.771 eV (S4) and 5.799 (S3) measured at 10 K, from which an effective lifetime (τ_{eff}) of about 0.75 ns is measured for both transition peaks, where τ_{eff} is defined as the time it takes for the emission intensity to decay from its

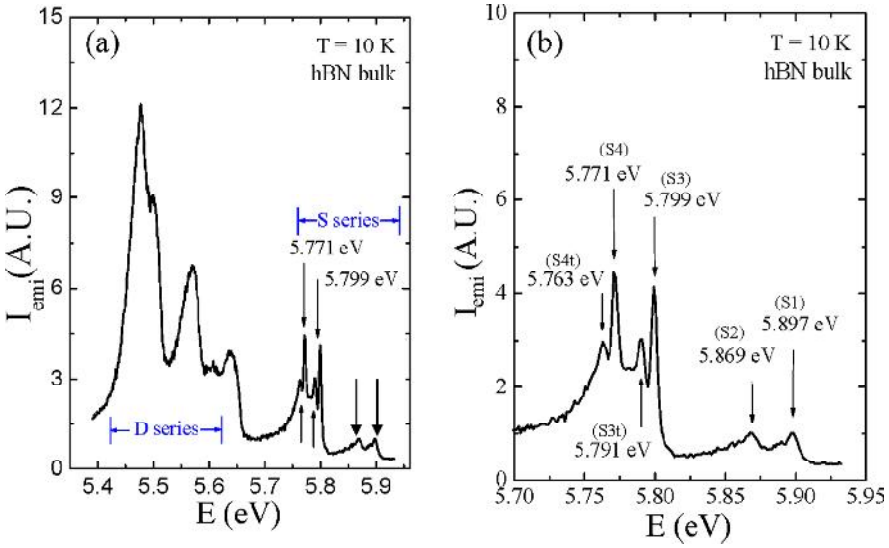

FIG. 2. A low temperature (10 K) photoluminescence emission spectrum of an *h*-BN bulk crystal (a) including both the free exciton (S-series) and bound-exciton (D-series) emission lines and (b) showing the fine features of the free exciton (S-series) emission lines.

maximum value A to A/e. It is noted that the measured subnanosecond lifetime is on the same order as the recombination lifetimes of excitons in wide bandgap semiconductors such as in GaN.[24] The results clearly reveal that the decay characteristics of these two emission lines are very similar, suggesting that these emission lines have the same origin.

The six transition lines of S-series can be described very well by a simple energy level diagram. In Fig. 4, we plot these six transition lines with their corresponding energy levels, where the widths of the vertical lines represent the relative emission intensities. The solid and dashed lines are used for the transitions with relatively strong and week emission intensities, respectively. Three pairs of transitions (S1/S2, S3/S4, S3t/S4t) can be distinguished from their similarities in intensity and linewidth. All the observed transitions and correlations between different emission lines become apparent from this diagram. Three different energy splitting levels of about 98 meV, 28 meV, and 8 meV can be identified. We believe that all these energy levels can be attributed to the phonon energies of different modes.

Based on previous experimental and theoretical studies,[25,26] we attribute the energy level of 98 meV to the A_{2u} phonon mode, an out-of-plane vibration at the center of the Brillouin zone (BZ) of *h*-BN. This means that the emission lines at 5.799 eV (S3)/5.771 eV (S4) are related to the 5.897 eV(S1)/5.869 eV (S2) emission lines through one A_{2u} phonon of about 98 meV. From the emission intensities, it appears that the S1 and S2 emission lines are absorbing one A_{2u} phonon of 98 meV of those of S3 and S4 emission lines, although the possibility of the reverse case of S3 and S4 emission lines being phonon replicas (emitting one A_{2u} phonon of 98 meV) of those of S1 and S2 emission lines cannot be precluded. In either cases, the situation is different from the typical optical transitions involving phonons in semiconductors, which usually emit phonons and therefore the phonon replica emission lines are located at lower energy positions with smaller emission intensities than their zero phonon counterparts. Very large electron–phonon interaction in *h*-BN has been previously inferred.[25–28] Other than the strong exciton–phonon interaction, the excitation photon energies used for the PL measurements in our case here (~6.28 eV) and in the case of Ref. 15 (~6.26 eV) are also near the energy band gap of *h*-BN, which may enhance the

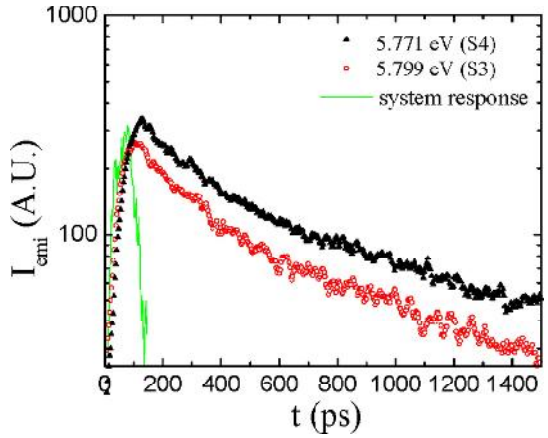

FIG. 3. Decay characteristics of S4 (5.771 eV) and S3 (5.799 eV) emission lines measured at 10 K. The system response is also included (green solid curve).

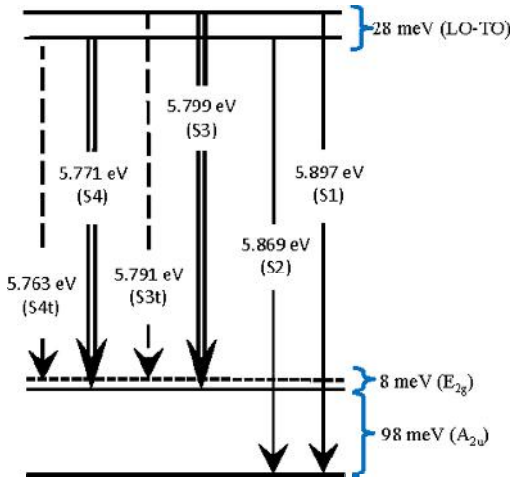

FIG. 4. Energy level diagram constructed for the S-series lines in the free exciton (FX) transition observed in *h*-BN. The thick solid lines indicate the emission lines with strong intensities while the dotted lines indicate emission lines with weak intensities.

emission intensities of the phonon-assisted lines due to the resonant Raman scattering process.

The emission lines between 5.799 eV (S3) and 5.771 eV (S4) as well as between 5.897 (S1) and 5.869 eV (S2) are separated by 28 meV, which are apparently also correlated. This energy separation may be accounted for by the LO-TO energy splitting at the center of the BZ.[26,27,29] A value of LO-TO splitting of $\sim 240\,\mathrm{cm}^{-1} \approx 30$ meV has been previously identified, which was attributed to the antisymmetric combination of the high-energy in-plane mode that is infrared active.[27] Furthermore, from the similarity of the spectral line shapes and energy separation, it appears that the emission lines of 5.799 eV (S3) and 5.791 eV (S3t) are also correlated with each other. The same is also true for the emission lines of 5.771 (S4) and 5.763 eV (S4t). The cause of this 8 meV splitting may be attributed to the E_{2g} mode (in-plane) phonon corresponding to the vibration of the whole *h*-BN sheet. Values of 6.5 meV and 6.4 meV for the E_{2g} mode phonon energy of low frequency have been previously deduced, respectively, from a theoretical calculation and Raman scattering experiment.[25,30] This phonon, related to the two BN planes slide against each other, has been termed as a "rigid-layer shear mode."[30] From the relative emission intensities, the 5.763 eV (S4t) and 5.791 eV (S3t) emission lines are, respectively, one phonon replicas (emitting one E_{2g} phonon of 8 meV) of the 5.771 eV (S4) and 5.799 eV (S3) emission lines. The small discrepancy between the E_{2g} phonon energy observed here (8 meV) and that reported earlier (6.4 meV) may be due to the fact that pyrolytic boron nitride (p-BN) was used previously,[30] whereas *h*-BN bulk crystal is used in the present study.

It is important to point out that the three phonon modes (98 meV, 28 meV, and 8 meV) identified are all associated with the Γ point (the center of the BZ). Based on these observations, we suggest that the emission line at 5.799 eV (S3) corresponds to the direct intrinsic FX transition in *h*-BN with zero phonon involved, while all other emission lines in the S-series are phonon-assisted lines, as illustrated in Fig. 4. On the other hand, it is equally possible that the emission line at 5.897 (S1) corresponds to the principal (zero phonon) FX transition in *h*-BN, while all other emission lines in the S-series are phonon replicas of the S1 emission line. Based on the similarity between the D- and S-series transitions shown in Fig. 2(a), we believe that the strong exciton-phonon coupling discussed above for FX may also be applicable to impurity-bound excitons.

In summary, the nature of exciton transitions in *h*-BN has been investigated by deep UV PL measurements. The results revealed significant differences in the basic optical emission properties between *h*-BN and other III-nitride semiconductors. Based on the separations between the energy peak positions of the FX emission lines, time-resolved PL results, and the known phonon modes in *h*-BN, we suggest that the fine features (S-series lines) in the free exciton transition are all related to one principal intrinsic transition line via the involvement of phonons of three different modes, which are associated with the center of the Brillouin zone. Our results thus offer a plausible alternative but simple picture for the understanding of the fundamental exciton transitions in *h*-BN.

The efforts on *h*-BN material growth are supported by DHS ARI Program (No. 2011-DN-077-ARI048), the studies of the fundamental optical properties of *h*-BN are supported by DOE (DE-FG02-09ER46552), and the studies of the basic structural properties of *h*-BN are supported by NSF (ECCS-1402886). Jiang and Lin are grateful to the AT&T Foundation for the support of Ed Whitacre and Linda Whitacre endowed chairs.

[1]R. W. Lynch and H. G. Drickamer, J. Chem. Phys. **44**, 181 (1966).
[2]S. L. Rumyantsev, M. E. Levinshtein, A. D. Jackson, S. N. Mohammmad, G. L. Harris, M. G. Spencer, and M. S. Shur, in *Properties of Advanced Semiconductor Materials GaN, AlN, InN, BN, SiC, SiGe*, edited by M. E. Levinshtein, S. L. Rumyantsev, and M. S. Shur (John Wiley & Sons, Inc., New York, 2001), pp. 67–92.
[3]Y. Kubota, K. Watanabe, O. Tsuda, and T. Taniguchi, Science **317**, 932 (2007).
[4]K. Watanabe, T. Taniguchi, and H. Kanda, Nat. Mater. **3**, 404 (2004).
[5]K. Watanabe, T. Taniguchi, and H. Kanda, Nat. Photonics **3**, 591 (2009).
[6]Y. Kobayashi, K. Kumakura, T. Akasaka, and T. Makimoto, Nature **484**, 223 (2012).
[7]R. Dahal, J. Li, S. Majety, B. N. Pantha, X. K. Cao, J. Y. Lin, and H. X. Jiang, Appl. Phys. Lett. **98**, 211110 (2011).
[8]S. Majety, J. Li, X. K. Cao, R. Dahal, B. N. Pantha, J. Y. Lin, and H. X. Jiang, Appl. Phys. Lett. **100**, 061121 (2012).
[9]J. Li, R. Dahal, S. Majety, J. Y. Lin, and H. X. Jiang, Nucl. Instrum. Methods Phys. Res., Sect. A **654**, 417 (2011).
[10]T. C. Doan, S. Majety, S. Grendadier, J. Li, J. Y. Lin, and H. X. Jiang, Nucl. Instrum. Methods Phys. Res., Sect. A **748**, 84 (2014); **783**, 121 (2015).
[11]T. Sugino, K. Tanioka, S. Kawasaki, and J. Shirafuji, Jpn. J. Appl. Phys., Part 2 **36**, L463 (1997).
[12]A. Zunger, A. Katzir, and A. Halperin, Phys. Rev. B **13**, 5560 (1976).
[13]X. K. Cao, B. Clubine, J. H. Edgar, J. Y. Lin, and H. X. Jiang, Appl. Phys. Lett. **103**, 191106 (2013).
[14]J. Li, K. B. Nam, M. L. Nakarmi, J. Y. Lin, H. X. Jiang, P. Carrier, and S.-H. Wei, Appl. Phys. Lett. **83**, 5163 (2003).
[15]K. Watanabe and T. Taniguchi, Phys. Rev. B **79**, 193104 (2009).
[16]B. Arnaud, S. Lebègue, P. Rabiller, and M. Alouani, Phys. Rev. Lett. **96**, 026402 (2006).
[17]B. Arnaud, S. Lebègue, P. Rabiller, and M. Alouani, Phys. Rev. Lett. **100**, 189702 (2008).
[18]L. Wirtz, A. Marini, M. Gruning, C. Attaccalite, G. Kresse, and A. Rubio, Phys. Rev. Lett. **100**, 189701 (2008).
[19]L. Wirtz, A. Marini, and A. Rubio, Phys. Rev. Lett. **96**, 126104 (2006).
[20]S. Majety, X. K. Cao, J. Li, R. Dahal, J. Y. Lin, and H. X. Jiang, Appl. Phys. Lett. **101**, 051110 (2012).
[21]X. Z. Du, J. Li, J. Y. Lin, and H. X. Jiang, Appl. Phys. Lett. **108**, 052106 (2016).
[22]T. B. Hoffman, B. Clubine, Y. Zhang, K. Snow, and J. H. Edgar, J. Cryst. Growth **393**, 114 (2014).
[23]R. S. Pease, Acta Cryst. **5**, 356 (1952).
[24]G. D. Chen, M. Smith, J. Y. Lin, H. X. Jiang, S.-H. Wei, M. Asif Khan, and C. J. Sun, Appl. Phys. Lett. **68**, 2784 (1996).
[25]J. Serrano, A. Bosak, R. Arenal, M. Krisch, K. Watanabe, T. Taniguchi, H. Kanda, A. Rubio, and L. Wirtz, Phys. Rev. Lett. **98**, 095503 (2007).
[26]R. Geick, C. H. Perry, and G. Rupprecht, Phys. Rev. **146**, 543 (1966).
[27]S. Reich, A. C. Ferrari, R. Arenal, A. Loiseau, I. Bello, and J. Robertson, Phys. Rev. B **71**, 205201 (2005).
[28]L. Museur, G. Brasse, A. Pierret, S. Maine, B. Attal-Tretout, F. Ducastelle, A. Loiseau, J. Barjon, K. Watanabe, T. Taniguchi, and A. Kanaev, Phys. Status Solidi RRL **5**, 214 (2011).
[29]G. Cassabois, P. Valvin, and B. Gil, "Hexagonal boron nitride is an indirect bandgap semiconductor," Nat. Photonics (published online, 2016).
[30]R. J. Nemanich, S. A. Solin, and R. M. Martin, Phys. Rev. B **23**, 6348 (1981).